Long-Range Electronic Coupling in Bis(cyclometalated) Ruthenium Complexes

Cendrine Patoux,[†] Jean-Pierre Launay,*[,†] Marc Beley,[‡] Sandrine Chodorowski-Kimmes,[‡] Jean-Paul Collin,*[,‡] Stuart James,[‡,§] and Jean-Pierre Sauvage[‡]

Contribution from the Molecular Electronics Group, CEMES, CNRS, 29 rue Jeanne Marvig, 31055 Toulouse Cedex, France, and Laboratoire de Chimie Organo-Minérale, Institut de Chimie, Université Louis Pasteur, 1 rue Blaise Pascal, 67008 Strasbourg, France

Received December 5, 1997

Abstract: Symmetrical and unsymmetrical ligands containing terpyridyl coordinating units (N, N, N) or a cyclometalating equivalent (N, C, N), connected back-to-back either directly or via a *p*-terphenylene or 1,3-phenylene spacer, have been used to construct new diruthenium complexes. These compounds incorporate various terdentate chelates as capping ligands, to allow a double control of the electronic properties of each subcomplex and of the ensemble: via the terminal ligand or through the bridging fragment. Electronic coupling was studied from the intervalence transitions observed in several bimetallic ruthenium complexes of the bis-(cyclometalated) type differing by the substitution of a nitrogen atom by carbon in the terminal terpyridyl unit. The largest metal−metal interaction was found in complexes for which the terminal complexing unit is of the 1,3-di-2-pyridylbenzene type, i.e., with the carbon atom located on the metal−metal C_2 axis of the molecule. Investigations of the mechanism of interaction by extended Hückel calculations showed that the replacement of nitrogen by carbon raises the filled ligand levels, increasing the mixing with ligand orbitals and thus the metal−metal coupling. Finally, the intervalence transition was still observed for a bridging ligand containing three phenylene units as spacers, corresponding to a 24-Å metal−metal distance.

Introduction

Intramolecular electron transfer between two metal sites linked by an organic ligand can be easily followed by the study of intervalence transitions.[1] In previous papers, we have studied bimetallic ruthenium complexes linked by ligands of either the bis(terpyridine) type[2] (**1,** cf. Figure 1) or the bis(cyclometalated) type (**2**).[3] It was found that the metal−metal coupling was much higher in the second kind of complexes, which was tentatively assigned to "a better orbital matching" between ruthenium and ligand orbitals. However, no detailed investigation of the interaction mechanism was performed at that time.

Since then, several new compounds of the cyclometalated type, with the connecting carbon atom located in different positions, have been prepared (**3**−**6** in Figure 1). All compounds reported here have the same general structure, each ruthenium atom being coordinated to two different ligands: a bridging ligand on one side and a terminal capping ligand on the other side. Thus we have first described compound **2** with the carbon atom on the bridging ligand in central position ("central" meaning on the metal−metal C_2 axis). Later Constable et al. described compound **4**, in which the carbon atom is located on the terminal ligand, in a lateral position[4] ("lateral" meaning outside the metal−metal C_2 axis of the molecule). More recently, we have synthesized compounds **3** and **5**, in which the carbon atoms lie on the binary axis of the molecule but either both on the terminal ligands or one on the bridging and one on the terminal ligand. Finally, Constable et al. reported compound **6**, where the carbon atoms are on the bridging ligand in the lateral position.[5]

This large variety of structures allows now a sharper discussion of the effect of C/N substitution. We have thus systematically studied intervalence transitions and the corresponding metal−metal couplings V_{ab} obtained through Hush's formula[6] for the above structures. The mechanism of metal−metal coupling through the bridging ligand has been enlighted by means of extended Hückel calculations. Finally, starting from the most favorable structure (**2**), we have investigated the cases of compound **7**, where the metal−metal distance reaches 24 Å, and compound **8**, where the connection on the central phenylene spacer is of the meta type.

[†] CNRS, Toulouse.

[‡] Université Louis Pasteur.

[§] Present address: Department of Chemistry, Imperial College, South Kensington, London SW7 2AY, U.K.

(1) See for instance the following reviews: Crutchley R. J. *Adv. Inorg. Chem.* **1994**, *41*, 273−325. Creutz, C. *Prog. Inorg. Chem.* **1983**, *30*, 1−73. See also: (a) Benniston, A. C.; Goulle, V.; Harriman, A.; Lehn, J.-M.; Marczinke, B. *J. Phys. Chem.* **1994**, *98*, 7798−7804. (b) Haga, M.-a.; Ali, Md. M.; Koseki, S.; Fujimoto, K.; Yoshimura, A.; Nozaki, K.; Ohno, T.; Nakajima, K.; Stufkens, D. J. *Inorg. Chem.* **1996**, *35*, 3335−3347. (c) Elliot, M. E.; Derr, D. L.; Ferrere, S.; Newton, M. D.; Liu, Y.-P. *J. Am. Chem. Soc.* **1996**, *118*, 5221−5228.

(2) Collin, J.-P.; Lainé, P.; Launay, J.-P.; Sauvage, J.-P.; Sour, A. *J. Chem. Soc., Chem. Commun.* **1993**, 434−435

(3) Beley, M.; Chodorowski-Kimmes, S.; Collin, J.-P.; Lainé, P.; Launay, J.-P.; Sauvage, J.-P. *Angew. Chem., Int. Ed. Engl.* **1994**, *33*, 1775−1778.

(4) Constable, E. C.; Cargill Thompson, A. M. W.; Greulich, S. *J. Chem. Soc., Chem. Commun.* **1993**, 1444−1446.

(5) Constable, E. C.; Cargill Thompson, A. M. W. *New J. Chem.* **1996**, *20*, 65−82.

(6) Hush formula: $V_{ab} = \{[2.05 \times 10^{-2}(\epsilon_{max}\bar{\nu}_{max}\Delta\bar{\nu}_{1/2})^{1/2}]/R\}$, where ϵ_{max}, $\bar{\nu}_{max}$, and $\Delta\bar{\nu}_{1/2}$ are, respectively, the molar extinction coefficient, the wavenumber at the maximal absorbance, and the bandwidth at half-maximum, while R is the metal−metal distance. Hush, N. S. *Prog. Inorg. Chem.* **1967**, *8*, 391−444. Hush, N. S. *Coord. Chem. Rev.* **1985**, *64*, 135−157. A recent critical discussion (Creutz, C.; Newton, M. D.; Sutin, N. *J. Photochem. Photobiol. A: Chem.* **1994**, *82*, 47−59) shows that this equation is still valid for strongly coupled systems, close to the class III limit.

S0002-7863(97)04137-1 CCC: $15.00
Published on Web 04/04/1998

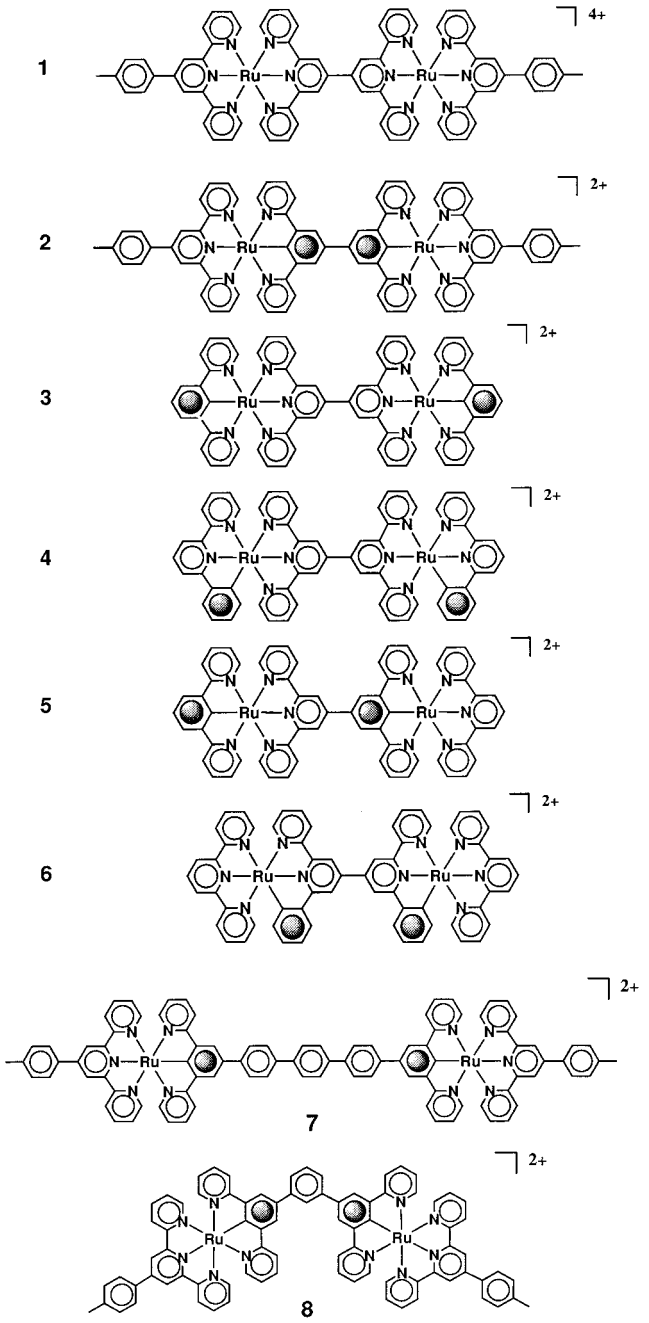

Figure 1. Structure of the studied compounds **1**−**8**.

Results and Discussion

Synthesis of Ligands. The precursor ligands involved in the ruthenium complexes are represented in Chart 1. The new ligand tpy-dpbH (tpy = terpyridine, dpb = dipyridylbenzene) was prepared in two steps as shown in the bottom of Chart 1.

Synthesis of Complexes. Three different strategies have been used to prepare the homodinuclear ruthenium complexes described in this study. An example for each strategy is depicted in Chart 2. (i) The first was based on the initial synthesis of the central bridging ligands and terminal ligands. The formation of a ruthenium moiety at each site of the bridging ligand can be simultaneous or sequential. This method allows the achievement of the symmetrical complexes **1** and **6** and the asymmetrical complex **5**. (ii) The second strategy leads to the dinuclear complexes by oxidative (compound **2**) or reductive (compounds **3** and **4**) coupling reactions as previously described in the literature.[7,8] (iii) The third strategy uses ruthenium(II) complexes as building blocks[9] in an aromatic cross-coupling reaction (Suzuki's procedure) between a diboronic derivative and a brominated ruthenium complex (compounds **7** and **8**).[10]

Chart 1

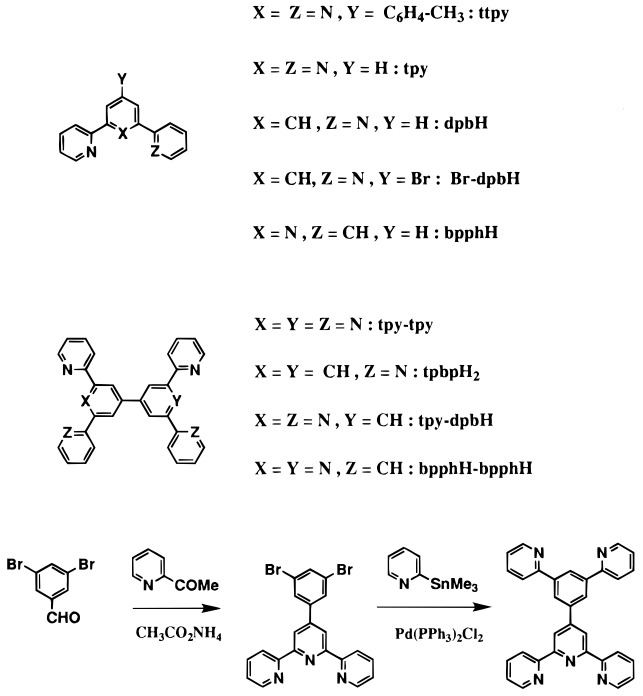

Chart 2

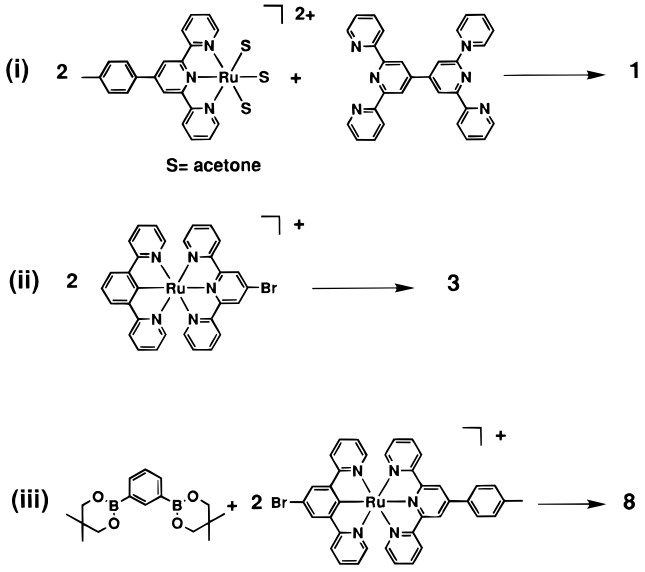

Experimental Electronic Couplings in the Different Cyclometalated Compounds. Since all studied compounds contain two ruthenium(II/III) redox centers, two oxidation processes are anticipated:

(7) Beley, M.; Collin, J.-P.; Louis, R.; Metz, M.; Sauvage, J.-P. *J. Am. Chem. Soc.* **1991**, *113*, 8521−8522.

(8) Barigelletti, F.; Flamigni, L.; Balzani, V.; Collin, J.-P.; Sauvage, J.-P.; Sour, A.; Constable, E. C.; Cargill Thompson, A. M. W. *J. Chem. Soc., Chem. Commun.* **1993**, 942−944.

(9) Tzalis, D.; Tor, Y. *J. Chem. Soc., Chem. Commun.* **1996**, 1043−1044.

(10) Chodorowski-Kimmes, S.; Beley, M.; Collin, J.-P.; Sauvage, J.-P. *Tetrahedron Lett.* **1996**, *37*, 2963−2966.

$$\text{Ru(II)}-\text{Ru(II)} - e^- \rightleftarrows \text{Ru(II)}-\text{Ru(III)} \qquad (E^\circ_1)$$

$$\text{Ru(II)}-\text{Ru(III)} - e^- \rightleftarrows \text{Ru(III)}-\text{Ru(III)} \qquad (E^\circ_2)$$

However, if the two standard redox potentials E°_1 and E°_2 are too close, a single two-electron wave is observed, with minor differences in shape with respect to a true bielectronic process. The different species are connected by the comproportionation equilibrium

$$\text{Ru(II)}-\text{Ru(II)} + \text{Ru(III)}-\text{Ru(III)} \rightleftarrows 2\text{Ru(II)}-\text{Ru(III)} \qquad (K_c)$$

K_c being determined by the difference $\Delta E^\circ = E^\circ_2 - E^\circ_1$. Differential pulse voltammetry allows a relatively accurate determination of ΔE° (and thus K_c) even in these circumstances.[11] The results are gathered in Table 1. In the series of compounds **1**−**6** derived from bis(terpyridine), K_c can vary from 15 (one wave) to 690 (two waves). Thus the metal−metal distance is not of course the only parameter determining K_c.

Experimental results about the intervalence transitions (position, extinction coefficient, width) are gathered in Table 2, and some representative spectra are given in Figure 2. Bandwidths are generally of the order of magnitude predicted by Hush theory,[6] except for **2** (narrower) and **8** (wider). In the case of **2**, this could be due to the strong electronic coupling (see below), which introduces some class III (delocalized)[1] character. Nevertheless, Hush's equation has been used since its range of application appears to be larger than previously believed.[6] For **8**, no obvious explanation for the bandwidth has been found. The experimental V_{ab} values obtained from Hush's equation,[6] and theoretical V_{ab} values from extended Hückel calculations are given in Table 2. Theoretical V_{ab} values are obtained from the splitting between molecular orbitals exhibiting high weights on ruthenium atoms and opposite parities (cf. Figure 3).

Experimental V_{ab} values vary widely in the series **1**−**6** and follow more or less the same trend as K_c values. (K_c variations are not the subject of the present work; detailed discussions on the relation between K_c and electronic coupling can be found elsewhere).[12] If we start from the bis(terpyridine) compound **1** as reference compound, most cyclometalated compounds give higher couplings. However, structure **2**, in which the carbon atoms are on the bridging ligand and in central position (i.e., on the C_2 axis of the molecule), is the best for the transmission of electronic interaction. By contrast, in compound **3**, where the carbon atoms are also on the C_2 axis, but located on the terminal ligand, the coupling is much lower, i.e., the same as in **1**. Compound **5** has structural features coming from both **2** and **3**, and as a matter of consequence, its coupling is intermediate. Finally, for compound **4**, where the carbon atoms are on the terminal ligand and in "lateral" position, we find a moderate V_{ab} coupling. In fact, compound **4** was already described by Constable et al.[4] In our study, we find 5000 mol^{-1} L cm^{-1} as the extinction coefficient by several independent determinations. Thus it seems that the position of the carbon atom in the N_5C sets plays an important role in determining the magnitude of the coupling.

Orbital Interpretation of Electronic Couplings. Electronic couplings and their variations can be addressed by quantum mechanical calculations. Ideally, one should use ab initio or semiempirical SCF (CNDO, INDO) methods,[13] but these treatments are too delicate to use for large molecules. It has been shown[14] that, in a number of cases, V_{ab} values can be correctly reproduced from extended Hückel calculations, using the "dimer splitting" method, i.e., the splitting between molecular orbitals with high weights on ruthenium atoms and different symmetries. (This method has been also used by Larsson[15] and Marcus et al.[16]).

To reduce calculation times, we have replaced in all the present study the tolylterpy (ttpy) terminal ligand by a terpyridine. Compounds were built and minimized using the Cerius2 software.[17] Using compounds **1** and **2** as references, we found that the main features of the molecular geometry were correctly reproduced (in particular, Ru−C bonds near 1.96 Å[7] and Ru−N bonds near 1.99 Å[18]), but not the central C−C distance (1.42 Å instead of 1.51 Å in the X-ray structure of $\mathbf{2}^{2+}$[7]) nor the dihedral angle between the pyridyl or phenylene rings of the bridging ligand (36° vs 22° from X-ray). But anyway, the exact structure may depend on the ruthenium oxidation state, as observed in the case of the bimetallic complexes of 3,3′,5,5′-tetrakis((*N*,*N*-dimethylamino)methyl)biphenylene ("bis-pincer") for which the Ru(III)−Ru(III) form exhibits a central C−C at 1.43 Å and a 0° dihedral angle, while for the Ru(II)−Ru(II) complex the figures are 1.47 Å and 36°.[19] Thus, in the present case, since we are dealing with a mixed valence compound, we have chosen a somewhat intermediate geometry with the central C−C distance adjusted "by hand" to 1.51 Å but the dihedral angle kept at 36°. Compounds **7** and **8** present more than one C−C bond connecting phenyl rings, and thus many possible conformations with almost equal energies. For **7**, we have chosen a conformation with alternate positive and negative dihedral angles, but it appeared that other conformations (e.g., helicoïdal) gave the same couplings. For **8**, we have imposed the conformation in which the external cyclometalated units are rotated in opposite directions so as to avoid each other as much as possible. In both cases (**7** and **8**), the dihedral angle was fixed at 36° and the C−C distance between phenyl rings at 1.51 Å.

Table 1. Electrochemical Data[a]

complex	E°_1 (V)	E°_2 (V)	K_c
1 (one wave)	1.27	1.34	15
2 (two waves)	0.34	0.505	690
3 (one wave)	0.51	0.578	15
4 (two waves)	0.52	0.66	222
5 (two waves)	0.46	0.61	422
6	0.62[b]		
7 (one wave)	0.48	0.49	4
8 (one wave)	0.48	0.54	10

[a] Standard redox potentials (V vs SCE) from differential pulse voltammetry with curve fitting and comproportionation constant computed from ΔE°. [b] Reference 5.

(11) Richardson, D. E.; Taube, H. *Inorg. Chem.* **1981**, *20*, 1278−1285.
(12) Sutton, J. E.; Taube, H. *Inorg. Chem.* **1981**, *20*, 3125−3134. Ernst, S.; Kasack, V.; Kaim, W., *Inorg. Chem.* **1988**, *27*, 1146−1148. Salaymeh, F.; Berhane, S.; Yusof, R.; de la Rosa, R., Fung, E. Y.; Matamoros, R.; Lau, K. W.; Zheng, Q.; Kober, E. M.; Curtis, J. C. *Inorg. Chem.* **1993**, *32*, 3895−3908.
(13) See the review by Newton: Newton, M. D. *Chem. Rev.* **1991**, *91*, 767−792.
(14) Joachim, C.; Launay, J.-P.; Woitellier, S. *Chem. Phys.* **1990**, *147*, 131−141.
(15) Larsson, S. *J. Am. Chem. Soc.* **1981**, *103*, 4034−4040. Larsson, S. *J. Chem. Soc., Faraday Trans. 2* **1983**, *79*, 1375−1388. Larsson, S. *J. Phys. Chem.* **1984**, *88*, 1321−1323.
(16) Siddarth, P.; Marcus, R. A. *J. Phys. Chem.* **1990**, *94*, 2985−2989.
(17) Cerius2, Biosym/Molecular Simulations, San Diego, CA.
(18) Cambridge Structural Database: Allen, F. H.; Kennard, O.; Taylor, R. *Acc. Chem. Res.* **1983**, *16*, 146.
(19) Steenwinkel, P. Thesis, Utrecht University, 1998. This work suggests that the planarity of the biphenylene ligand is caused by the Ru(III)−Ru(III) oxidation states distribution, which favors quinoidal forms. Thus, in a mixed valence complex, the biphenylene moiety is not expected to be planar.

Table 2. Parameters of the Intervalence Transitions (Maximum Wavelength, Full Width at Half-Maximum, Maximum Extinction Coefficient) and Experimental and Theoretical Couplings for Compounds **1**−**8**

complex	λ_{max} (nm)	$\Delta\bar{\nu}_{1/2}$ (cm^{-1})	ϵ_{max} (M^{-1} cm^{-1})	$V_{ab\ exp}$ (eV)	$V_{ab\ calcd}$[a] (eV)	$V_{ab\ calcd}$[b] (eV)	$V_{ab\ calcd}$[c] (eV)
1	1580	4008	1620	0.047	0.065	0.042	0.145
2	1936	2665	22000	0.127	0.061	0.098	0.264
3	1585	5146	1227	0.046	0.063	0.039	
4	2468	5709	5036	0.078	0.067	0.037	
5	2360	5374	3648	0.066	0.063	0.061	
6					0.062	0.041	
7	985	7500	924	0.028	0.003	0.021	
8	1848	6503	270	0.018	0.001	0.010	

[a] Calculated for Ru(4d) at −11.23 eV (extended Hückel). [b] Calculated for Ru(4d) at −12.5 eV (extended Hückel). [c] From ZINDO (see text).

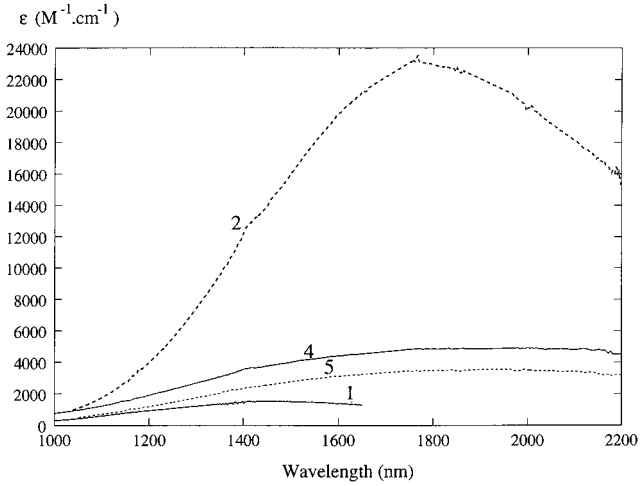

Figure 2. Some representative intervalence spectra, corrected from comproportionation. The numbers on the curves correspond to the different compounds.

(i) Variation in V_{ab} Coupling between 1 and 2. We first concentrate on the main experimental fact, which is the large V_{ab} variation between **1** and **2**, i.e., upon N/C replacement on the bridging ligand in the central position. A crucial problem is the parametrization of Ru(4d) orbital energies, and in the past, we have used Tatsumi and Hoffmann's value,[20] i.e. −11.23 eV, this figure coming from their study on $Ru(NH_3)_6^{2+}$. However, in the present case, the large difference in coupling between **1** and **2** could not be reproduced, the calculation giving a slight decrease from **1** to **2**, while experimentally there is an increase of 170% (see Table 2). A systematic investigation of the influence of the Ru(4d) orbital energy then revealed a curious behavior: for Ru(4d) above −11.23 eV (e.g., −10.5 eV), the effect was reversed, i.e., higher couplings were obtained for **1**, instead of **2**. Conversely, when the energy of the Ru(4d) orbitals was decreased with respect to −11.23 eV, the effect of C/N substitution increased, and for Ru(4d) at −12.5 eV, the right order of magnitude of the couplings was obtained with a large increase in V_{ab} (ca. 130%) when replacing N by C^-. Thus it appears that the −11.23 eV value is very close to a singularity and that the choice of the Ru(4d) orbital energy is crucial.

To get more insight on this problem and avoid a too arbitrary choice, we have performed comparative INDO/1 calculations on **1** and **2** using the ZINDO package.[21] Since INDO/1 is a SCF calculation with explicit treatment of electron−electron repulsion, it can be hoped that the metal orbital energies are more correctly defined than in the extended Hückel method and, in particular, are able to vary from one compound to another. INDO/1 calculations were performed on closed shell systems, i.e., for the Ru(II)−Ru(II) state,[22] and the V_{ab} couplings extracted from the splitting between filled molecular orbitals, as for the extended Hückel procedure.[14] Although V_{ab} values are much higher than experimental ones or extended Hückel ones (see Table 2), the marked increase in coupling between **1** and **2** is reproduced. We have checked that this result remains valid for a large range of input parameters.[23] The problem of the Ru(4d) energies can now be addressed on a more rigorous basis, by inspection of the Fock matrix. This matrix determines the molecular orbitals after SCF convergence. Thus the diagonal terms can be considered as the best definition of atomic orbital energies in a given compound, taking into account electronic repulsions. It is found that INDO/1 calculations locate Ru(4d) orbitals clearly below C(2p) orbitals, as the extended Hückel method does for −12.5 eV, but not for −11.23 eV (see Figure 4).

Thus we consider that the extended Hückel calculation with Ru(4d) at −12.5 eV is a reasonable choice,[24] with the advantage of giving straightforwardly realistic V_{ab} values. This choice proved in addition convenient for reproducing the weak couplings in **7** and **8** (see Table 2). The following discussion will thus be based on extended Hückel calculations.

The comparison of bis(terpyridine) with bis(dipyridylbenzene) as ligands shows that, upon replacement of N by the isoelectronic C^-, there is a general increase in the energy of the molecular orbitals (Figure 5). The energy of the ruthenium(4d) orbitals being close to the ligand HOMO energy, a better orbital mixing can be anticipated in the cyclometalated compound. However, another effect can be imagined: due to the higher σ-donor strength of the carbon ligand,[25] one can expect

(20) Tatsumi, K.; Hoffmann, R. *J. Am. Chem. Soc.* **1981**, *103*, 3328−3341.

(21) ZINDO: Zerner, M. C. Quantum Theory Project, University of Florida, Gainesville, FL. ZINDO 96.0: Molecular Simulations, San Diego, CA.

(22) Attempts to perform open shell calculations, corresponding to the Ru(II)−Ru(III) (d^6−d^5) actual electronic structure of the mixed valence compounds, failed for reasons of non-SCF convergence. We attribute this difficulty to the proximity of the six molecular orbitals obtained from combinations of d_{xy}, d_{xz}, and d_{yz} ruthenium levels, resulting in quasi-degeneracy of the different energy states when there is one hole with respect to the d^6−d^6 configuration. In addition, since there is no absolute definition of orbital energies for open shell calculations, a rigorous calculation would have to rely on the total energy with inclusion of configuration interaction, which represents a formidable quantum chemistry problem for such large molecules.

(23) Although the INDO/1 method is less arbitrary than extended Hückel, there remains some empirical parameters to choose. The main ones are the ionization potentials, which are different according to the considered electronic configuration (s^2d^{n-2}, s^1d^{n-1}, s^0d^n, or even a mixture of all these), and the β parameters, which are used to determine the off-diagonal elements in the Fock matrix. However, in our case, orbital energies were only weakly affected by the choice of the Ru β parameter.

(24) Before quoting the −11.23 eV figure, a value of −14.9 eV was given by Thorn and Hoffmann (Thorn, D. L.; Hoffmann, R. *Inorg. Chem.* **1978**, *17*, 126−140) for the Ru(4d) energy. Thus the present choice of −12.5 eV is not unrealistic.

(25) Watts, R. J. *Comments Inorg. Chem.* **1991**, *11*, 303. Maestri, M.; Balzani, V.; Deuschel-Cornioley, Ch.; von Zelewski, A. *Adv. Photochem.* **1992**, *17*, 1.

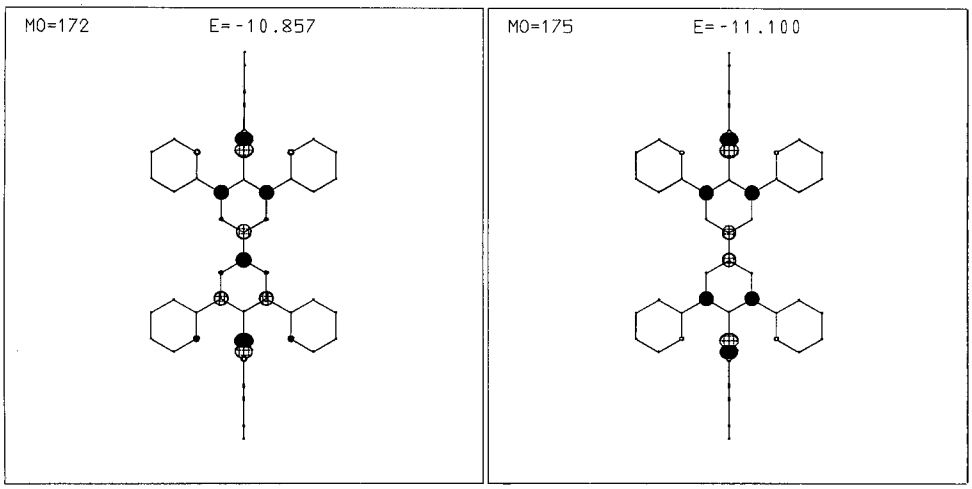

Figure 3. Orbitals defining the V_{ab} coupling in compound **2**. For sake of simplicity, **2** has been drawn in a "flat" conformation, which does not alter qualitatively the shape of the orbitals.

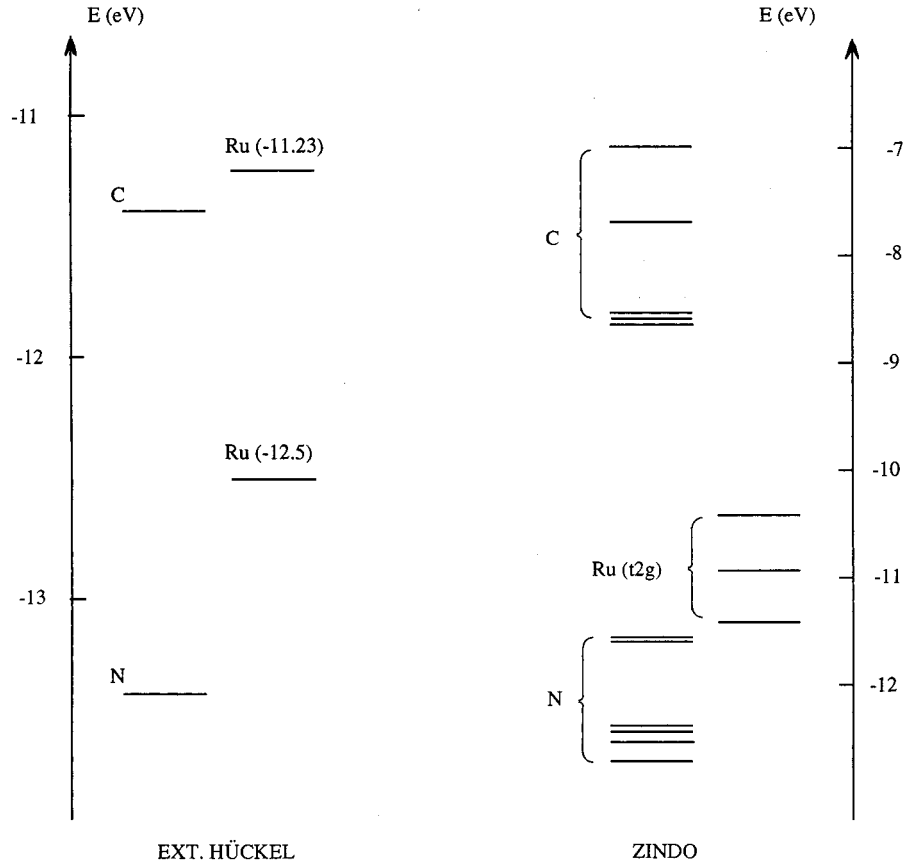

Figure 4. Positions of the Ru(4d) orbital energies with respect to C(2p) and N(2p), from extended Hückel (left) and ZINDO (right). In the case of ZINDO, a sampling of energy levels taken from the Fock matrix is given, since all orbitals of the same kind no longer have the same energy. Although the energy scales are different, the relative positions of orbitals can be compared (see text).

some transfer of electron density on the metal with a concomitant increase of the ruthenium orbitals energies. This is indeed suggested by the shift in the electrochemical redox potential of the ruthenium(II/III) couple, which decreases by ca. 0.7 V upon substitution of N by C^-.[26] Such an orbital shift should *decrease* the mixing of metal orbitals with the ligand HOMO but, on the other hand, would increase the mixing with ligand LUMO. However, as explained above, increasing the energy of ruthenium(4d) orbitals does not reproduce correctly the gross behavior, and thus, in the following, the possible σ effect of C^- on ruthenium energies will be neglected.

A detailed examination of molecular orbitals of complex **2** reveals that ruthenium 4d orbitals have indeed mixed more efficiently with the ligand HOMO than with the LUMO. This is consistent with the appearance of an intense and low-energy ligand-to-metal charge-transfer transition (LMCT) when the complex is oxidized to the ruthenium(III) state.[26] When comparing the molecular orbitals in **2** and in the corresponding free bridging ligand, the interaction can be rationalized as follows (see Figure 6): the two d_{xz} orbitals of the ruthenium atoms,

(26) Beley, M.; Collin, J.-P.; Sauvage, J.-P. *Inorg. Chem.* **1993**, *32*, 4539−4543.

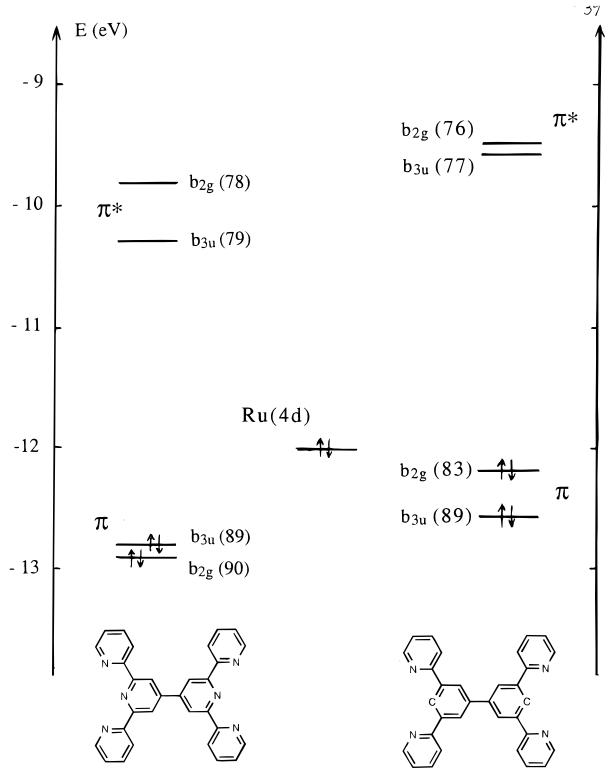

Figure 5. Respective energetic positions of the ligand π and π^* MO in **1** and **2** and of the ruthenium (4d) orbitals. The diagram is limited to b_{2g} and b_{3u} orbitals.

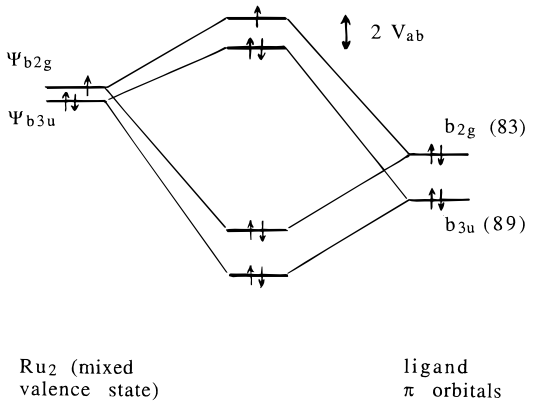

Figure 6. Interaction of the Ψ_{b2g} and Ψ_{b3u} symmetry combinations with ligand π orbitals. The scheme corresponds to the case of compound **2**, but energies are not to scale.

which have the right symmetry to interact with the π system of the ligand, can be combined, taking into account the molecular symmetry (D_{2h}) to give

$$\Psi_{b_{2g}} = \frac{1}{\sqrt{2}}(d_{xz}^{A} + d_{xz}^{B}) \quad (1)$$

$$\Psi_{b_{3u}} = \frac{1}{\sqrt{2}}(d_{xz}^{A} + d_{xz}^{B}) \quad (2)$$

At this stage, due to the large distance between the ruthenium sites, the direct metal−metal coupling is very small and the orbital splitting between the above symmetry combinations is practically zero. However, their interaction with ligand orbitals of the same symmetry lifts the degeneracy. In particular, the free ligand exhibits π orbitals with b_{2g} (no. 83) and b_{3u} (no. 89) symmetries at markedly different energies. Thus, their mixings

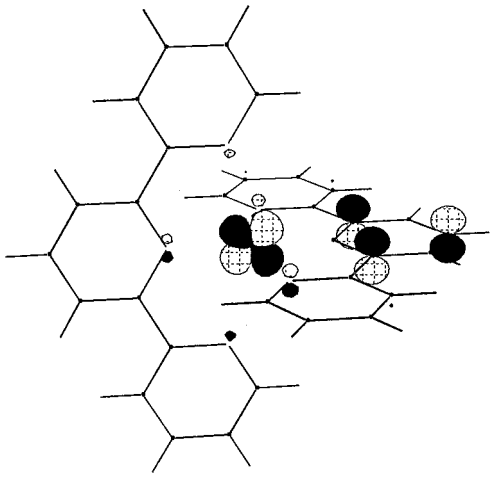

Figure 7. Shape of the HOMO in $[(tpy)Ru(dpb)]^+$

with the metal combinations (1) and (2) are different and a splitting of the final levels results (Figure 6).

Another way to interpret the electronic coupling is to consider the properties of a $[(tpy)Ru^{II}(dpb)]^+$ fragment (dpb = dipyridylbenzene), i.e., one-half of molecule **2**. Since ruthenium(II) (t_{2g}^6) has an electron pair available for back-bonding with dpb, it is formally analogous to a donor substituent such as $-NH_2$. Thus the HOMO of this fragment is essentially a d_{xz} orbital with some contributions on the phenyl ring in ortho and para positions (see Figure 7; note that there is almost no contribution from the lateral pyridine rings). Incidentally, this electronic structure explains nicely the formation mechanism of **2** from $[(tpy)Ru^{II}(dpb)]^+$: since it is formed upon oxidative coupling,[7,26] we may assume that the oxidation of Ru(II) to Ru(III) generates appreciable unpaired electron density at the para position, so that a radical coupling occurs associated to a deprotonation process. Returning now to the mechanism of electronic interaction, when two fragments such as $[(tpy)Ru^{II}(dpb)]^+$ are associated to give **2**, the previous HOMOs can combine across the central C−C bond in either a bonding or antibonding way, which gives the orbital splitting defining the V_{ab} coupling (see Figure 3).

A consequence of this interpretation is that the V_{ab} coupling should be determined by the HOMO coefficient in the para position for the $[(tpy)Ru^{II}(dpb)]^+$ fragment. In fact, we found that a qualitative study at the simple Hückel level of the effect of substitution on an aromatic ring could explain the main trends. A very simple model simulating the consequences of cyclometalation is thus the following: we start from a pyridine ring with a heteroatomic substituent attached to the nitrogen atom (see Figure 8). To the heteroatom (playing the role of ruthenium) we first assign a Coulomb integral equal to that of carbon. When replacing N by C, i.e., going from a pyridine complex to an organometallic compound, it is found that the coefficient of the HOMO at the para position does not change. If now we move downward the Coulomb integral of the heteroatom to 0.5 (in β units), the replacement of N by C produces a much larger effect (Figure 8), the electron density at the para position being multiplied by ca. 2.8. *Thus, the particular properties of cyclometalated complexes with respect to terpyridyl complexes come from the fact that the ruthenium orbitals are slightly below C(2p) orbitals.* Since in the extended Hückel method C(2p) orbitals are located at −11.4 eV, it is now clear why ruthenium orbitals should be located at −12.5 eV rather that −11.23 eV to reproduce the experimental behavior. This stresses again that the major interaction is

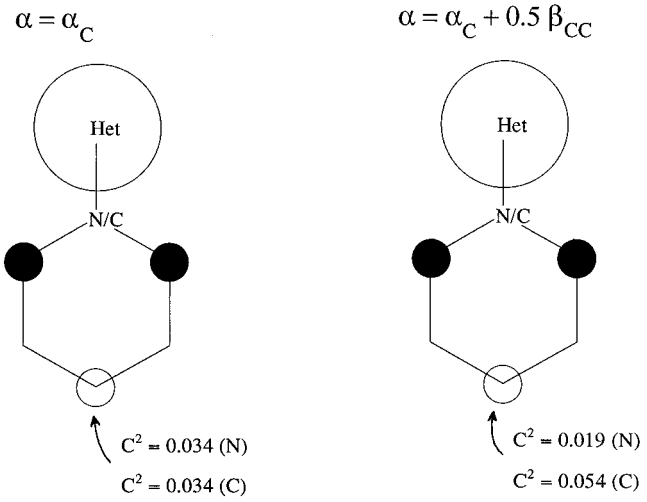

Figure 8. Simple Hückel model showing how much electronic effects are transmitted in the para position. The heteroatom simulates ruthenium. The square of the HOMO coefficient is given for two values of the heteroatom Coulomb integral.

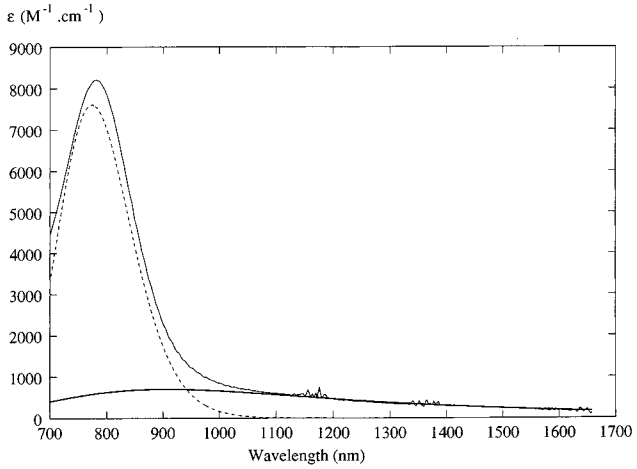

Figure 9. Corrected spectrum of the mixed valence form of **7** with deconvolution in two bands. The band at 800 nm is assigned to the ferricinium chromophore present in the mixed valence species, while the intervalence band is the weak and broad band culminating near 900 nm.

between ruthenium orbitals and the filled orbitals of ligands. Recent work reported by Crutchley et al. shows the efficiency of this kind of interaction to promote strong metal−metal coupling.[27] A similar effect could explain the strong metal−metal coupling observed in ruthenium complexes of the "bis-pincer" family, where "pincer" = bis((dimethylamino)methyl)-aryl moiety.[28]

(ii) Effect of the *σ*-Aryl Position. Expanding now the theoretical interpretation to the other compounds, we note in Table 2 that most V_{ab} couplings are correctly reproduced by the extended Hückel calculation with Ru(4d) at −12.5 eV. Logically, for **3**, the coupling is found to be the same as for **1** because the carbon atoms are on the terminal ligands. For **5**, the coupling is found intermediate between those of **1** and **2**, since there is only one carbon on the bridging ligand. In the case of **4**, the calculation predicts almost no change with respect to **1**, which agrees with intuition because the carbon atoms are on the terminal ligands. But the experimental value shows a noticeable increase (see Table 2). This disagreement between experiment and calculation could be due to subtle effects not reproduced at the extended Hückel level. Alternately we may consider an experimental artifact because in **4** the intervalence transition occurs at a particularly long wavelength with a large bandwidth.

Compound **6** has been recently described by Constable and Cargill Thompson.[5] No intervalence band has been reported, but we can compute a V_{ab} coupling of 0.041 eV, which is close to the computed value for **1**. Since most of the electronic interaction is transmitted through the aromatic ring located on the C_2 axis of the molecule, it is not surprising that substitution on a lateral ring has a very small effect on the coupling.

(iii) Very Long Distance Intervalence Electron Transfer (7). Since the best structure for efficient transmission of electron interaction is **2**, we have expanded the previous cyclometalated series[3] by studying compound **7**, in which three phenylene groups are intercalated between the dipyridylphenyl terminal units. Ruthenium atoms are separated by a total of five rings, and the metal−metal distance amounts to 24 Å. The intervalence transition appears as a very broad tail on the edge of a nearby charge-transfer transition (Figure 9), but deconvolution was possible and yielded V_{ab} = 0.028 eV (Table 2). To our knowledge, this is one of the intervalence transitions involving electron transfer over the longest distance.[29] The theoretical V_{ab} value (0.021 eV) is close to the experimental one. Incidentally, this value was found to be independent of the detailed conformation, provided the dihedral angles between phenylene rings were kept at the same value.

(iv) Meta Connection (8). In the same spirit as above, the cyclometalated structure of type **2** can be used to probe electron transfer across a phenyl ring with a meta connection (compound **8**). Initially, structure **8** was devised to test the possibilities of controlling electron transfer by suitable substitutions on the central phenyl ring. The observed V_{ab} is the smallest reported in Table 2 (0.018 eV), with again a rather good agreement with the theoretical value. A parallel experimental and theoretical study performed on diferrocenylbenzenes[30] explains the weakness of the interaction.

Conclusion

The present study has shown that the best structure for a high metal−metal coupling is the one in which the terminal complexing unit is of the dpb⁻ type, i.e., with the carbon atom located on the metal−metal C_2 axis of the molecule. This is logical since quantum calculations show that the interaction is transmitted along the most direct path, i.e., by mixing mainly with the central rings located between the metal atoms. The experimental V_{ab} values and their variations with N/C substitution are correctly reproduced by extended Hückel calculations, provided that Ru(4d) energies are empirically adapted to a slightly different value with respect to published figures. This adjustment can be at least qualitatively justified by semiempirical calculations (INDO). In addition, extended Hückel calculations

(27) Rezvani, A. R.; Bensimon, C.; Cromp, B.; Reber, C.; Greedan, J. E.; Kondratiev, V. V.; Crutchley, R. J. *Inorg. Chem.* **1997**, *36*, 3322−3329 and references therein.

(28) Sutter, J.-P.; Grove, D. M.; Beley, M.; Collin, J.-P.; Veldman, N.; Spek, A. L.; Sauvage, J.-P.; van Koten, G. *Angew. Chem., Int. Ed. Engl.* **1994**, *33*, 1282−1285.

(29) Intervalence transitions over comparable distances have been also observed with organic mixed valence systems (Bonvoisin, J.; Launay, J.-P.; Rovira, C.; Veciana, J. *Angew. Chem., Int. Ed. Engl.* **1994**, *33*, 2106−2109), but in organic redox sites, the definition of distance is not as clear as here because the initial and final wave functions are delocalized on more than one atom. A recent example by Lehn et al. describes an intervalence transition over a similar distance (24 Å) in a bimetallic system.[1a]

(30) Patoux, C.; Coudret, C.; Launay, J.-P.; Joachim, C.; Gourdon, A. *Inorg. Chem.* **1997**, *36*, 5037−5049.

allow the "mapping" of the crucial orbitals defining the coupling, leading to a better understanding of the mechanism of interaction. Finally, for the most favorable structure, an intervalence transition has been observed for a particularly long distance (24 Å), the main limitation for larger distances being the increased mixing with a nearby charge-transfer transition.

Experimental Section

Instrumentation. ^{1}H NMR spectra were acquired on a Bruker WP200 SY instrument. Mass spectra were obtained by using VG ZAB-HF and Thomson THN 208 mass spectrometers.

Starting Organic Compounds. 3,5-Dibromobenzaldehyde,[31] 4′-tolyl-2,2′:6′,2″-terpyridine[32] (ttpy), 4′-bromo-2,2′:6′,2″-terpyridine[33] (tpy-Br), 3,5-dipyridylbenzene[7] (dpbH), and 1-bromo-3,5-dipyridylbenzene[34] (dpbH-Br) were prepared according to literature procedures.

1,3-Dibromo-5-terpyridylbenzene. 3,5-Dibromobenzaldehyde (6.3 g, 23.8 mmol), 2-acetylpyridine (5.8 g, 47.7 mmol), ammonium acetate (27.3 g, 0.34 mol), and acetamide (42 g, 0.7 mol) were heated at reflux (160 °C) for 2 h. The solution was then allowed to cool to 110 °C, and aqueous NaOH (20.7 g in 45 mL of H_2O) was added over 15 min. The mixture was again heated at reflux (120 °C) for 2 h, then allowed to cool until a black precipitate solidified. The supernatant was decanted. The black residue was washed with water, then extracted with CH_2Cl_2 and filtered. The filtrate was evaporated to dryness to leave a black tar, which was preadsorbed on alumina and subjected to columm chromatography on alumina with 5% Et_2O in hexane and 10% Et_2O in hexane as eluents, to give 1.35 g of impure product. The impure ligand was dissolved in CH_2Cl_2 (30 mL), and a Mohr salt [$FeSO_4(NH_4)_2SO_4 \cdot 6H_2O$] aqueous solution (0.54 g in 10 mL of H_2O) was added. The violet solution was stirred for 10 min and CH_2Cl_2 removed. A solution of KPF_6 (0.5 g in 10 mL H_2O) was added. The resulting precipitate was filtered and then dissolved in CH_3CN (20 mL) and toluene (100 mL). The volume was reduced to 50 mL to give a precipitate which was filtered and washed with toluene (40 mL) and pentane (40 mL) to leave 1.26 g of purple crystals. The ligand was then decomplexed from the iron by heating the purple product with a mixture of CH_3CN (50 mL) and aqueous NaOH (50 mL, 1M) at 40 °C for 10 mn. The CH_3CN was removed and the remaining aqueous suspension filtered. The solid was washed with water (40 mL) and recrystallized from CH_2Cl_2/EtOH to give 0.87 g (8%) of an off-white powder.

^{1}H NMR (200 MHz, CD_2Cl_2): δ 8.72 (d, 2H, 1.5 Hz), 8.64 (s, 2H), 8.65 (d, 2H, 8 Hz), 8.02 (d, 2H, 2 Hz), 7.86 (dd, 2H, 8 and 1.2 Hz), 7.79 (t, 1H, 2 Hz), 7.39 (dd, 2H, 8 and 1.2 Hz).

1,1-Dipyrido-5-terpyridylbenzene (tpy-dpbH). *tert*-Butyllithium (2.14 mmol, 1.5 M solution in pentane) was added to a stirred solution of 2-bromopyridine (0.17 g, 1.07 mmol) in THF (5 mL) over 6 min at −78 °C. The resulting yellow solution was stirred at −78 °C for 20 min, and $ZnCl_2$ (0.145 g, 1.07 mmol, predried under vacuum at 150 °C for 2 h) was added in one batch. The mixture was then allowed to warm to room temperature to give a red solution. 1,3-Dibromo-5-terpyridylbenzene (0.1 g; 0.214 mmol) and Pd $(PPh_3)_4$ (0.025 g, 0.02 mmol) were added, and the mixture was heated to reflux for 66 h. The solvents were removed, and the residue was stirred with CH_2Cl_2 (10 mL) and aqueous KOH (5 mL, 2 M) for 30 min, after which the layers were separated and the aqueous phase again extracted with CH_2Cl_2 (40 mL). The extracts were combined and the solvent removed. The residue was then preadsorbed on alumina and subjected to column chromatography on alumina with an Et_2O−hexane mixture (50:50) as the eluent to give a white powder (25 mg, 25%).

^{1}H NMR (200 MHz, CD_2Cl_2): δ 8.88 (s, 2H), 8.77 (t, 1H, 1.66 Hz), 8.75 (m, 4H), 8.69 (d, 4H, 8 Hz), 8.55 (d, 2H, 1.66 Hz), 7.99 (d, 4H, 8 Hz), 7.91 (dd, 2H, 6 and 1.8 Hz), 7.83 (dd, 2H, 8 and 1.8 Hz), 7.38 (dd, 2H, 8 and 1.2 Hz), 7.31 (dd, 2H, 8 and 1.2 Hz). MS: m/z = 463 ($C_{31}H_{21}N_5$ requires 463).

Bis(2,2-dimethyltrimethylene)-4,4″-terphenylylenediboronate (9). *tert*-Butyllithium (15 mmol, 1.5 M solution in pentane) was added under argon to a stirred solution of 4,4″-dibromoterphenyl (1.5 g, 3.85 mmol) in THF (50 mL) at −78 °C. After 1 h, the mixture was warmed to 0 °C for 30 min, then cooled to −78 °C. The green suspension was added via cannula to a solution of trimethylborate (0.8 g, 7.7 mmol) in THF at −70 °C. Stirring was continued for 15 h and the mixture allowed to warm to room temperature overnight. The yellow mixture was poured over ice (20 g), and then 2 mL of H_2SO_4 was added. Following removal of the THF, the diboronic acid was precipitated by addition of concentrated HCl. The product obtained was added to a solution of 2,2-dimethyl-1,3-propanediol (0.3 g, 2.8 mmol) in benzene and heated under reflux under a Dean−Stark head. After 2 h, evaporation of the benzene gave the diboronate as a pale yellow solid. It was recrystallized from a hexane−toluene mixture (390 mg, 22%).

^{1}H NMR (200 MHz, $CDCl_3$): δ 7.89 (d, 4H, 8.2 Hz), 7.70 (s, 4H), 7.64 (d, 4H, 8.2 Hz), 3.79 (s, 8H), 1.04 (s, 12H). Anal. Calcd for $C_{28}H_{32}B_2O_4$: C, 74.0; H, 7.1; B, 4.7. Found: C, 76.0; H, 7.5; B, 4.1. MS: m/z = 454 ($C_{28}H_{32}B_2O_4$ requires 454.2).

Bis(2,2-dimethyltrimethylene)-1,3-phenylylenediboronate (10). This compound was prepared following the method described by Cootts et al.[35]

^{1}H NMR (200 MHz, CD_2Cl_2): δ 8.35 (s, 1H), 7.83 (d, 2H, 9 Hz), 7.34 (t, 1H, 9 Hz), 3.77 (s, 8H), 1.02 (s, 12H). MS: m/z = 302. ($C_{16}H_{24}B_2O_4$ requires 302).

Complexes. 1,[2] **2**,[7] **4**,[8] **7**,[10] and **8**[10] were prepared as described previously. **3** was prepared by following the method described by Constable et al. for **4**.[8] Homocoupling of (dpb)Ru(tpy-Br)$^+$ in the presence of a Ni^0 phosphine complex and Zn dust in DMF afforded **3** in 77% yield.

^{1}H NMR (200 MHz, CD_3CN): δ 9.95 (s, 4H), 8.83 (d, 4H, 7.9 Hz), 8.32 (d, 4H, 7.6 Hz), 8.20 (d, 4H, 7.9 Hz), 7.85 (ddd, 4H, 7.9, 7.9 and 1.4 Hz), 7.67 (ddd, 4H, 7.9, 7.9 and 1.4 Hz), 7.52 (t, 2H, 7.6 Hz), 7.16 (m, 12H), 6.72 (dd, 4H, 6 and 6 Hz). FAB-MS (nitrobenzyl alcohol matrix): m-PF_6^- = 1275 ($C_{62}H_{42}N_{10}Ru_2PF_6$ requires 1275).

(dpb)Ru(tpy-Br)(PF_6) (11). This precursor was prepared in the same manner as for the analogous compound (dpb)Ru(ttpy)(PF_6)[7] from Ru(tpy-Br)Cl_3 and dpbH in 66% yield.

^{1}H NMR (200 MHz, CD_3CN): δ 8.95 (s, 2H), 8.42 (d, 2H, 8 Hz), 8.25 (d, 2H, 8 Hz), 8.13 (d, 2H, 8 Hz), 7.70 (ddd, 2H, 7.5, 7.5 and 1.5 Hz), 7.60 (ddd, 2H, 7.5, 7.5 and 1.6 Hz), 7.45 (t, 1H, 8 Hz), 7.13 (d, 2H, 4.7 Hz), 7.00 (m, 4H), 6.64 (ddd, 2H, 7.5, 7.5 and 1.4 Hz). FAB-MS (nitrobenzyl alcohol matrix): m-PF_6^- = 646 ($C_{31}H_{21}N_5BrRu$ requires 646).

(dpb)Ru(tpy-dpbH)(PF_6) (12). A mixture of $RuCl_2(PPh_3)_3$ (0.108 g, 112 μmol) and dpbH (26 mg, 112 μmol) in *n*-BuOH was refluxed under argon for 3 h. Ether (20 mL) was added to the cooled reaction mixture. The brown precipitate obtained was discarded by filtration. The filtrate was evaporated to dryness and the residue dissolved in EtOH (40 mL). To this solution was added the ditopic ligand tpy-dpbH (52 mg, 112 μmol). The reaction mixture was refluxed under argon for 3 h. After evaporation of EtOH, the residue was dissolved in CH_3CN (20 mL) and treated with an aqueous solution of KPF_6 (0.2 g in 40 mL). The precipitate obtained was washed with water (20 mL) and toluene (20 mL). The complex was purified by silica gel chromatography eluting with a mixture of CH_3CN and an aqueous solution of KNO_3 (96:4, KNO_3 0.5 M) (64 mg, 62%).

^{1}H NMR (200 MHz, CD_3CN): δ 9.1 (s, 2H), 8.93 (t, 1H, 1.6 Hz), 8.83 (d, 2H, 1.6 Hz), 8.74 (d, 2H, 6 Hz), 8.55 (d, 2H, 8 Hz), 8.1 (m, 6H), 7.95 (ddd, 2H, 7.5, 7.5 and 1.4 Hz), 7.66 (ddd, 2H, 7.5, 7.5 and 1.4 Hz), 8.75 (ddd, 2H, 7.5, 7.5 and 1.4 Hz, 7.46 (t, 1H, 8 Hz), 7.40 (ddd, 2H, 7.5, 7.5 and 1.4 Hz), 7.09 (d, 4H, 6 Hz), 6.92 (t, 2H, 8 Hz), 6.63 (t, 2H, 8 Hz). FAB-MS (nitrobenzyl alcohol matrix): m-PF_6 = 795.8 ($C_{47}H_{32}N_7Ru$ requires 796).

(31) Chen, L. S.; Chen, G. J.; Tamborski, C., *J. Organomet. Chem.* **1981**, *215*, 281.

(32) Collin, J.-P.; Guillerez, S.; Sauvage, J.-P.; Barigelletti, F.; De Cola, L.; Flamigni, L.; Balzani, V. *Inorg. Chem.* **1991**, *30*, 4230−4238.

(33) Constable, E. C.; Ward, M. D. *J. Chem. Soc., Dalton Trans.* **1990**, 1405−1409.

(34) Beley, M.; Chodorowski, S.; Collin, J.-P.; Sauvage, J.-P. *Tetrahedron Lett.* **1993**, *34*, 2933−2936.

(35) Cootts, I. G. C.; Goldschmid, H. R.; Musgrave, O. C. *J. Chem. Soc. C* **1970**, 488−493.

(dpb)Ru(tpy-dpbRutpy) (PF_6)$_2$ (5). A mixture of Ru(tpy)Cl_3 (44 mg, 100 μmol) and $AgBF_4$ (59 mg, 300 μmol) in acetone (10 mL) was refluxed for 2 h under air. After filtration, the solvent was evaporated and the mauve residue was dissolved in *n*-BuOH (10 mL). To this solution was added (dpb)Ru(tpy-dpbH)(PF_6) (83 mg, 88 μmol), and the solution was heated at 100 °C, under argon, for 7 h. After evaporation of *n*-BuOH, the residue was redissolved in CH_3CN (20 mL) and treated with an aqueous solution of KPF_6 (0.2 g in 40 mL). The precipitate obtained was washed with water (20 mL) and ether (20 mL). The complex was purified by silica gel chromatography (SiO_2, CH_3CN−aqueous KNO_3 mixture). After anionic exchange, **5** was obtained as a black powder (60 mg, 48%).

^{1}H NMR (200 MHz, CD_3CN): δ 9.46 (s, 2H), 9.14 (s, 2H), 8.80 (d, 2H, 8 Hz), 8.74 (d, 2H, 8 Hz) 8.170 (m, 2H), 8.50 (t, 4H, 8 Hz), 8.34 (t, 1H, 8 Hz), 8.00 (d, 2H, 8 Hz), 7.80 (m, 6H), 7.65 (ddd, 2H, 7.5, 7.5 and 1.4 Hz), 7.40 (d, 2H, 8 Hz), 7.23 (m, 9H): 7.04 (ddd, 2H, 7.5, 7.5 and 1.4 Hz), 6.76 (ddd, 2H, 7.5, 7.5 and 1.4 Hz), 6.61 (m, 2H). FAB-MS (nitrobenzyl alcohol matrix) *m*-PF_6^- = 1275 ($C_{62}H_{42}N_{10}Ru_2$ PF_6 requires 1275).

(ttpy)Ru(dpb-Br)(PF_6) (13). This compound was synthesized as described for (dpb)Ru(ttpy)(PF_6)[7] from Ru(ttpy)Cl_3 and dpbH−Br in 78% yield.

^{1}H NMR (200 MHz, CD_3CN): δ 8.99 (s, 2H), 8.56 (d, 2H, 8.2 Hz), 8.41 (s, 2H), 8.14 (m, 4H), 7.90 (m, 6H), 7.14 (m, 4H), 7.01 (td, 2H, 5.7 and 0.7 Hz), 6.71 (td, 2H, 5.7 and 1.6 Hz), 2.51 (s, 3H).

Electrochemistry. Cyclic voltammetry was performed with an Electromat 2000 system (ISMP Technologie) using a platinum wire as the working electrode and a saturated calomel electrode as the reference electrode. The solvent was acetonitrile, containing 0.1 M tetrabutylammonium hexafluorophosphate as the supporting electrolyte, and the standard scan rate was 0.1 V s^{-1}. Current potential curves were recorded with a rotating platinum disk electrode (Metrohm). Differential pulse voltammetry was performed with the same equipment, using a 48-mV pulse with a width of 50 ms and with 0.37 s between pulses. Positive feedback ohmic drop compensation was used, the solution resistance being determined by current interruption. $\Delta E°$, the difference in standard potentials for the two electrochemical processes, was determined from differential pulse voltammetry data by comparison with calculated curves.[11] Then, comproportionation constants (K_c) were determined using the relation

$$K_c = \exp\left(\frac{\Delta E° F}{RT}\right)$$

This method proved superior to the spectrophotometric method[36] used earlier for compounds **1** and **2**.

Spectroelectrochemistry and Determination of Metal−Metal Couplings. Intervalence transitions were recorded during controlled potential electrolysis in a special two-compartment electrolysis cell described elsewhere.[30] The working electrode was a platinum grid and the solvent acetonitrile containing 0.1 M tetrabutylammonium hexafluorophosphate. At given intervals, the electrolysis was stopped and the solution was transferred in a spectrophotometric flow cell (1-cm path length) with Teflon tubing by a syringe suction system. After spectrum recording, the solution was transferred back in the electrochemical cell and the electrolysis was resumed. UV−vis near-IR were recorded using a Shimadzu UV-PC 3101 spectrophotometer.

In a typical experiment, ca. 10 spectra were recorded in the course of oxidation of a Ru(II)−Ru(II) complex to the Ru(III)−Ru(III) state. This allowed an accurate location of the half-oxidation point, corresponding to the maximum concentration of the mixed valence species, in equilibrium with fully reduced and fully oxidized species. The initial, final and half-oxidation spectra were then combined, taking into account the comproportionation constant, to give the corrected spectrum of the mixed valence species. The corrected spectrum was then deconvoluted into Gaussian bands using a procedure already described.[36] Finally, the metal−metal coupling was computed from Hush's equation.[6]

Molecular Modeling and Quantum Chemical Calculations. Molecular geometry was optimized using the Cerius2 package.[17] A modification of the Dreiding 2.21 force field was used, with Ru−N bonds and Ru−C bonds defined by K_b = 700 kcal mol^{-1} Å^{-2} and R_0 = 2.04 Å (N) or 2.02 Å (C). A cosine harmonic term (θ_0 = 90°, K = 400 kcal) around ruthenium was introduced to avoid artifactual distortions (bending) of the ligands. In the case of **2**, after mimimization, the central C−C bond was fixed at the crystallographic value (1.51 Å).[7] Extended Hückel calculations were performed with the CACAO program of Mealli and Proserpio.[37] Ruthenium parameters were taken from Tatsumi and Hoffmann,[20] with initially the Ru(4d) orbitals located at −11.23 eV. This value was slightly modified during this study, as explained above. Electronic coupling values (V_{ab}) were obtained by the "dimer splitting" method,[14] i.e., from the splitting between two molecular orbitals with high weights on ruthenium atoms and different symmetries (Figure 3). A correction (according to eq 4 of ref 38) was used for the nonsymmetrical system **5**, for which V_{ab} is not directly one-half of the orbital splitting. ZINDO calculations[21] were performed on closed shell [Ru(II)−Ru(II)] molecules using s^0d^n ionization potentials and β_d = −15.0 eV for ruthenium, as advocated by Broo and Lincoln.[39]

Acknowledgment. This research has been supported by CNRS GDR 1009 "Electronique Moléculaire" and EC HCM network ERB CHR XCT 940538 "Electron and Energy Transfer in Model Systems". We also thank Dominique de Montauzon (Laboratoire de Chimie de Coordination, Toulouse) for electrochemical advice and facilities, Jacques Bonvoisin (CEMES) for software training, and Christophe Coudret (CEMES) for fruitful discussions.

JA974137+

(36) Ribou, A.-C.; Launay, J.-P.; Takahashi, K.; Nihira, T.; Tarutani, S.; Spangler, C. W. *Inorg. Chem.* **1994**, *33*, 1325−1329.

(37) CACAO PC Version 4.0 (July 1994): Mealli, C.; Proserpio, D. M. *J. Chem. Educ.* **1990**, *67*, 399−402.

(38) Woitellier, S.; Launay, J.-P.; Joachim, C. *Chem. Phys.* **1989**, *131*, 481−488.

(39) Broo, A.; Lincoln, P. *Inorg. Chem.* **1997**, *36*, 2544−2553.